PROCEEDINGS OF SCIENCE

Particle acceleration in neutron star ultra-strong magnetic fields

Pétri Jérôme

Université de Strasbourg, CNRS, Observatoire astronomique de Strasbourg, UMR 7550, 11 rue de l'université, F-67000 Strasbourg, France.

E-mail: jerome.petri@astro.unistra.fr

Neutron stars produce ultra-relativistic particles efficiently accelerated by their ultra strong electromagnetic fields, copiously radiation very high energy photons in the GeV/TeV range. However, no numerical code is able to handle such very high Lorentz factors and magnetic field strengths around the quantum critical limit of $4{,}4 \cdot 10^9$T. In this work, we study particle acceleration and radiation reaction damping in a magnetic dipole with magnetic field strengths as high as 10^{10}T, typical for magnetars. We investigated particle acceleration and the impact of radiation reaction for electrons, protons and iron nuclei. The maximum Lorentz factor depends on the particle species but only weakly on the magnetic field strength. Electrons reach energies up to $\gamma_e \approx 10^8 - 10^9$ whereas protons energies up to $\gamma_p \approx 10^5 - 10^6$ and iron up to $\gamma \approx 10^4 - 10^5$. While protons and irons are not affected by radiation reaction, electrons are drastically decelerated, reducing their maximum Lorentz factor by 2 orders of magnitude [10].

39th International Cosmic Ray Conference (ICRC2025)
15–24 July 2025
Geneva, Switzerland

PoS(ICRC2025)116

1. Introduction

Neutron stars are anchored with ultra-strong magnetic fields as high as $B_c \approx 4{,}4 \cdot 10^9$ T or even higher. For instance magnetars sustain field strengths well above this limit of B_c and are therefore able to accelerate particles to extreme energies with very high Lorentz factors of $\gamma \approx 10^9$. However, radiation reaction will drastically impact their trajectory. Strong fields and large Lorentz factors leads indeed naturally to strong radiation reaction of the charged particle motion that can be described by the Landau-Lifshitz approximation. Exact analytical solutions of this Landau-Lifshitz equation exist. For constant and uniform electromagnetic fields, the spatio-temporal derivatives vanish in the Landau-Lifshitz approximation and is sometimes called the reduced Landau-Lifshitz equation (LLR). We use this approximation to advance in time the position and velocity of charged particles.

In this paper [10] we study particle acceleration around a neutron star, using the exact scaling between the neutron star spin and the cyclotron frequency. In section 2 we recall the equation of motion as derived by Landau-Lifshitz and its exact analytical solution, the appropriate normalization and the algorithm. Section 3 describes an astrophysical application to neutron star electrodynamics and the upper limit of particle acceleration efficiency. Finally conclusions are drawn in section 4.

2. Equation of motion

The description of the self-force produced by an accelerated charge starts with the Lorentz-Abraham-Dirac equation (LAD) [1, 2, 4, 6]. Unfortunately this self-force leads to runaway solutions because the associated equation of motion is of third order in time. One approach to remedy this pitfall is the Landau-Lifshitz formulation, a perturbative expansion of the LAD equation [5]. Here, we adopt this point of view.

2.1 Landau-Lifshitz approximation

Landau-Lifshitz [5] derived an approximation valid in most astrophysical configurations, that is free of runaway instabilities. The equation of motion is

$$\frac{du^i}{d\tau} = \frac{q}{m} F^{ik} u_k + \frac{q\,\tau_\mathrm{m}}{m} g^i \tag{1a}$$

$$g^i = \partial_\ell F^{ik} u_k u^\ell + \frac{q}{m}\left(F^{ik} F_{k\ell} u^\ell + (F^{\ell m} u_m)(F_{\ell k} u^k)\frac{u^i}{c^2}\right) \tag{1b}$$

where q and m are the particle charge and rest mass, u^i its 4-velocity, τ its proper time, F^{ik} the electromagnetic or Faraday tensor, c the speed of light and τ_m the light crossing time across the particle classical radius r_m (within a factor unity) $\tau_\mathrm{m} = q^2/6\,\pi\,\varepsilon_0\,m\,c^3$. It is advantageous to express it in terms of the electron classical radius r_e crossing time amounting to $\tau_\mathrm{e} = 2\,r_\mathrm{e}/3\,c = 6{,}26 \cdot 10^{-24}$ s. The typical timescale for the radiation reaction is therefore $\tau_\mathrm{m} = \frac{2}{3}\frac{r_\mathrm{m}}{c} = \left(\frac{q^2/e^2}{m/m_\mathrm{e}}\right)\tau_\mathrm{e}$. For instance for protons, this time is three orders of magnitude less than for leptons $\tau_\mathrm{p} = \frac{m_e}{m_p}\tau_\mathrm{e} = 3{,}41 \cdot 10^{-27}$ s.

Interestingly, exact analytical solutions exist for eq.(1) in some special configurations of electromagnetic fields, time dependent or time independent. We use these analytical expressions to integrate the equation of motion.

2.2 Radiation reaction limit

In ultra-strong electromagnetic fields, radiation reaction plays an important role. In the asymptotic limit of ultra-relativistic motions, assuming that the radiation damping exactly balances the electric field acceleration, we can solve for the particle velocity [7] which is decomposed into an electric drift motion, interpreted as the velocity required to switch to a frame where the electric and magnetic field are aligned, and a motion along this common direction in this new frame. Denoting the velocity vector for positive charges as $\mathbf{v}_+$ and that for negative charges as $\mathbf{v}_-$, we find

$$\mathbf{v}_\pm = \frac{\mathbf{E}\wedge\mathbf{B} \pm (E_0\,\mathbf{E}/c + c\,B_0\,\mathbf{B})}{E_0^2/c^2 + B^2}. \tag{2}$$

Particles moving exactly at the speed of light. E_0 and B_0 are the strength of the electric and magnetic field in the frame where they are aligned. They are obtained from the electromagnetic invariants $\mathcal{I}_1 = \mathbf{E}^2 - c^2\,\mathbf{B}^2 = E_0^2 - c^2\,B_0^2$ and $\mathcal{I}_2 = c\,\mathbf{E}\cdot\mathbf{B} = c\,E_0\,B_0$. Imposing $E_0 \geq 0$ we find $E_0^2 = \frac{1}{2}\,(\mathcal{I}_1 + \sqrt{\mathcal{I}_1^2 + 4\,\mathcal{I}_2^2})$ and $c\,B_0 = \mathrm{sign}(\mathcal{I}_2)\,\sqrt{E_0^2 - \mathcal{I}_1}$.

3. Application to neutron stars

We apply our previous algorithms to realistic cases of rotating ultra magnetised neutron stars. The neutron star radius is fixed to $R_* = 12$ km. The accurate configuration of the electromagnetic field is taken from a rotating magnetic dipole in vacuum and given by [3].

3.1 Relevant parameters without dimension

We normalise the frequency to the stellar angular frequency $\omega = \Omega_*$ and considered three populations of neutron stars: young pulsars with period $P_* = 1$ s and surface magnetic field strengths $B_* = 10^8$ T, millisecond pulsars with period $P_* = 5$ ms and $B_* = 10^5$ T and magnetars with period $P_* = 10$ s and $B_* = 10^{10}$ T.

We distinguish three kind of particles: a first group crashing onto the stellar surface, a second group of trapped particles and a third group of escaping particles, all accelerated to high energies. Particles are considered trapped when they still have not crashed onto the surface or not yet escaped the light cylinder. Particles are placed regularly within the light-cylinder, starting at rest or with an initial velocity vector oriented along the magnetic field line, directed toward the star or towards infinity, with a Lorentz factor equal to $\gamma_0 = 10^3$ or starting at rest. The neutron star obliquity is set to $\chi = \{0°, 30°, 60°, 90°, 120°, 150°, 180°\}$. We found that the final results are not very sensitive to the initial Lorentz factor because charges are immediately accelerated in the direction of the electric field and therefore loose memory about their initial state. Our simulation results are thus summarized for particles starting at rest only. We simulated a total number of 48 particles for each neutron star type and each obliquity, spread around three radii r_0, right at the surface R_*, approximately half-way between the surface and the light-cylinder (a geometric average) and at the light cylinder, thus $r_0 = \{R_*, \sqrt{R_*\,r_\mathrm{L}}, r_\mathrm{L}\}$. For comparison we performed simulations with and without radiation reaction.

3.2 Orders of magnitude

Before presenting the accurate numerical simulations of particle trajectories and their radiation reaction in the vicinity of neutron stars, we remind the orders of magnitude of the maximum Lorentz factors expected when charges are accelerated in the electric potential produced by a rotating magnetized perfectly conducting star. The most optimistic view adopts the full potential drop between the pole and the equator as an estimate of the accelerating field thus

$$\gamma_{\rm max}^{\rm full} \approx \frac{q\,\Omega_*\,B_*\,R_*^2}{m\,c^2} = \frac{R_*}{r_{\rm L}}\,\frac{R_*}{r_{\rm B}} \tag{3}$$

where $r_{\rm B} = c/\omega_{\rm B}$ is the non relativistic Larmor radius. If the accelerating potential is only available across the polar caps as expected from nearly force-free magnetosphere models, the maximum energy corresponds to

$$\gamma_{\rm max}^{\rm pc} \approx \frac{q\,\Omega_*^2\,B_*\,R_*^3}{m\,c^3} = \left(\frac{R_*}{r_{\rm L}}\right)^2\,\frac{R_*}{r_{\rm B}} \approx \frac{R_*}{r_{\rm L}}\,\gamma_{\rm max}^{\rm full} \tag{4}$$

which is a factor $R_*/r_{\rm L}$ smaller than for the former case. Table 1 summarizes the maximum Lorentz factors for electrons, protons and irons around millisecond pulsars, young pulsars and magnetars. The values reported in this table for $\gamma_{\rm max}^{\rm full}$ are at best upper limits for the vacuum case. Only an accurate numerical integration of the equation of motion gives robust results as we now show.

Neutron star	$\log\gamma_{\rm max}^{\rm full}$ / $\log\gamma_{\rm max}^{\rm pc}$		
	electron	proton	iron
millisecond	10.5 / 9.3	7.3 / 6.0	7.0 / 5.7
young	11.2 / 7.7	8.0 / 4.4	7.7 / 4.1
magnetar	12.2 / 7.7	9.0 / 4.4	8.7 / 4.1

Table 1: Maximum Lorentz factor orders of magnitude from conservative arguments about neutron star magnetospheres. Values for full potential drops are given on the left of the "/" symbol and for polar cap potential drops on the right in logarithmic scale.

3.3 Escaping particles

Particles reaching distances larger than $10\,r_{\rm L}$ are reputed to be leaving the neutron star magnetosphere. The run halts when the particle reaches larger distances. Fig. 1 shows the distribution of Lorentz factor for electrons in green, protons in red and iron nuclei in blue, irrespective of the magnetic field inclination angle χ and for magnetars. The left column corresponds to a motion with radiation reaction (RR) whereas the right column to motion without radiation reaction. First, electrons are the most effectively accelerated particles reaching final Lorentz factors up to $\gamma_{\rm f} \sim 10^9$ in the LLR approximation for millisecond pulsars. This is however two orders of magnitude less than without radiation reaction where $\gamma_{\rm f} \sim 10^{11}$. Second, as expected protons and iron nuclei acquire much less energy, only about $\gamma_{\rm f} \sim 10^6$ for millisecond pulsars, wherever LLR is used or not. For young pulsars, electrons also reach $\gamma_{\rm f} \sim 10^9$ in the LLR regime instead of $\gamma_{\rm f} \sim 10^{11}$ for the pure Lorentz force. Protons and iron nuclei are much less subject to radiation reaction, showing no impact on the maximum Lorentz factor remaining at $\gamma_{\rm f} \sim 10^4 - 10^{4.5}$. For magnetars, radiation

reaction remains negligible irrespective of the nature of each species. Electrons reach energies up to $\gamma_f \sim 10^{7.5}$ whereas protons and iron nuclei $\gamma_f \sim 10^3 - 10^{3.5}$. Therefore, radiation reaction does not significantly perturb the trajectories of particles with lower charge over mass ratio q/m. Contrary to electrons, protons and irons do not suffer from radiation friction.

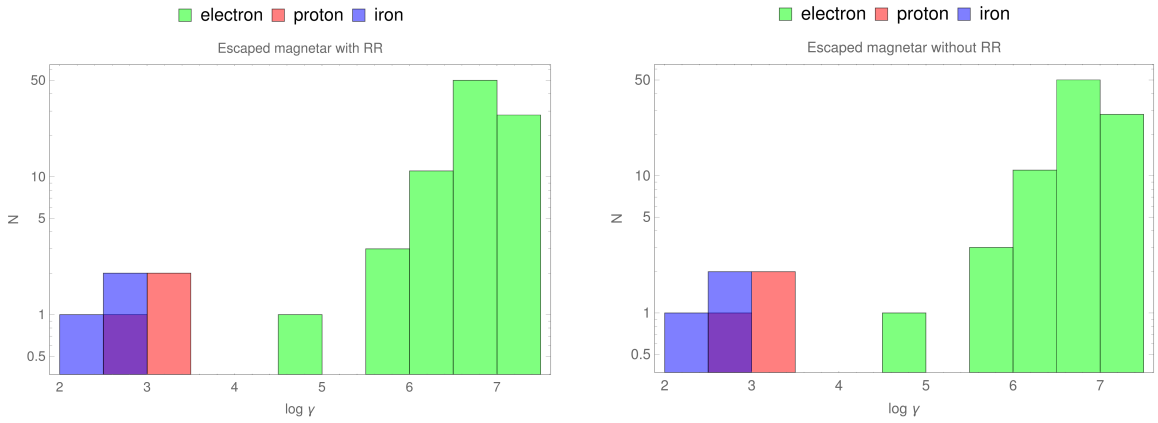

Figure 1: Distribution of escaped particles for magnetars. Electron Lorentz factors are shown in green, proton in red and iron nuclei in blue. The left column includes radiation reaction (RR) whereas the right panel does not.

3.4 Crashed particles

Closer to the star, most species quickly crash onto the surface in a time much shorter than the neutron star spin period. Particles crashing onto the neutron star surface are easily recognized by the fact that their final position lies inside the star. Compared to escaping particles, the situation is now reversed, magnetars offering the highest energetic particles heating the surface and millisecond pulsars the lowest energetic particles, see left column of Fig. 2. This is accounted for by the lower surface magnetic field of millisecond pulsars, being three to five orders of magnitude lower than young pulsars or magnetars respectively. Neglecting radiation reaction , electrons are able to reach Lorentz factors up to $\gamma_f \sim 10^{11}$ for magnetars but only $\gamma_f \sim 10^{8.5}$ for millisecond pulsars. The radiation reaction impact is strongest for magnetars. However, protons and irons are not perturbed by radiation reaction except sensibly for magnetars. Nevertheless, we observe that with radiation reaction protons remain the most energetic particles with final Lorentz factors about $\gamma_f \sim 10^{7.5} - 10^{8.5}$ irrespective of the neutron star nature, millisecond, young or magnetar. For electrons the situation is drastically different. They radiate copiously, decreasing they Lorentz factor by three orders of magnitude comparing to the no radiation reaction case in the magnetar environment. The decrease is less pronounced for young or millisecond pulsars but still perceptible.

3.5 Trapped particles

By default, we assume that trapped particles are those not crashing onto the neutron star and not escaping to large distances outside the light cylinder within the simulation time span corresponding to several neutron star periods. Fig. 3 summarizes the distribution of Lorentz factors for electrons,

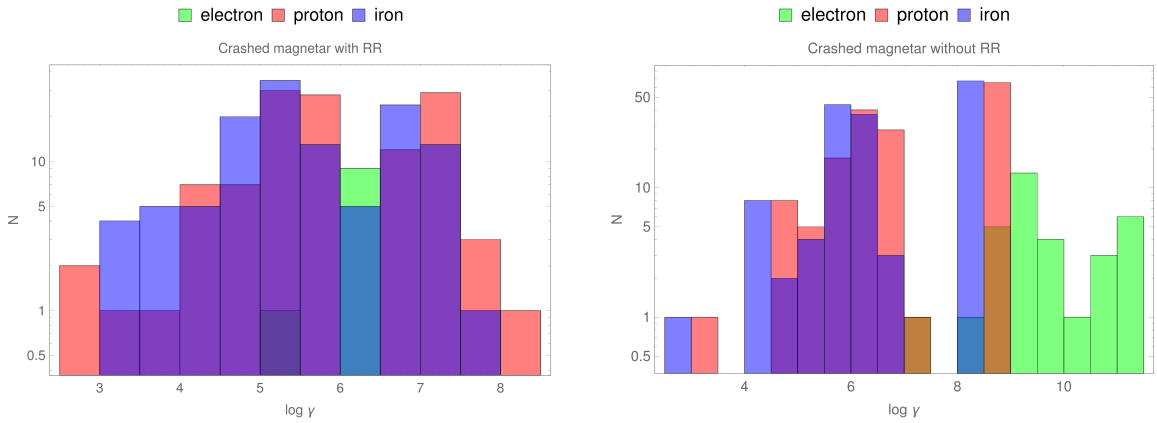

Figure 2: Same as Fig. 1 but for crashed particles.

protons and irons in the LLR approximation and without radiation reaction. Protons and irons are still insensitive to radiation reaction except for magnetars. Electrons are much more sensitive to radiation reaction, decreasing their Lorentz factor by four orders of magnitude for millisecond pulsars, young pulsars and magnetars. Millisecond pulsars produce trapped protons and irons with energies about $\gamma_f \sim 10^7$ whereas young pulsars and magnetars one decade more up to $\gamma_f \sim 10^8$, no matter if radiation reaction is included or not. Electrons are trapped with similar Lorentz factor although slightly less for millisecond pulsars.

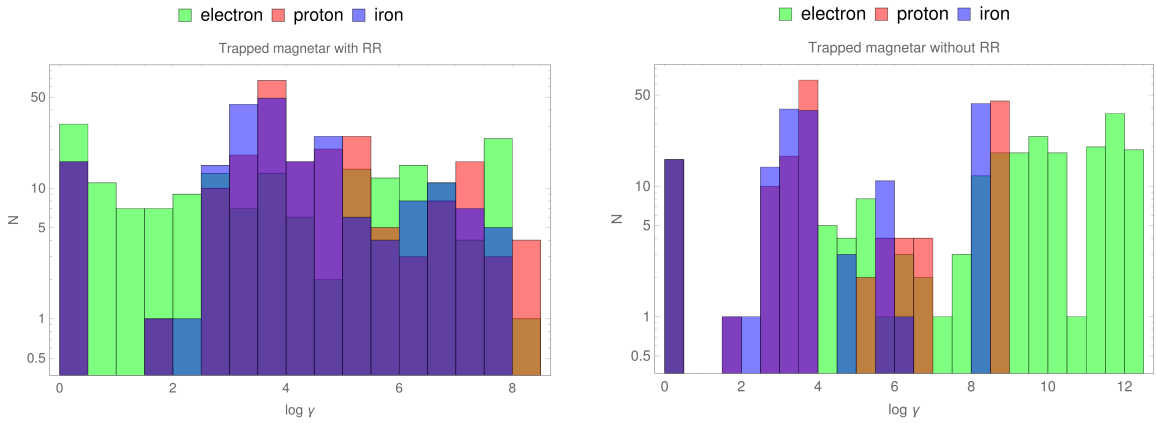

Figure 3: Same as Fig. 1 but for trapped particles.

3.6 Maximum Lorentz factor

For escaping particles, in the wave zone, the gain in energy is limited by the spherical nature of the electromagnetic field, meaning decreasing in strength with distance like $1/r$. For a null like electromagnetic field [9] showed that this severely limits the maximum Lorentz factor to values of

$$\gamma_{\max} \approx 2\,(a_{B_L}/\pi)^{2/3} \tag{5}$$

a_{B_L} being the strength parameter as measured at the light cylinder. Radiation reaction remains also negligible in this wave zone. Table 2 summarizes the relevant parameters at the light cylinder

for the three kinds of neutrons stars. As a rule of thumb, we found no particle with Lorentz factor exceeding $\gamma_f \approx 10^{9.1}$ in the LLR regime. Because the vacuum electromagnetic used in our simulations corresponds to the one producing the strongest parallel electric field (with respect to the magnetic field), no particle should be created and moving with Lorentz factor higher than $10^{9.1}$ within the magnetosphere. Eq. (5) is satisfied for non null like electromagnetic waves as those

Neutron star	$\log a_{B_L}$	$\log \gamma_{max}$		
		Crashed	Trapped	Escaped
millisecond	9.3 / 6.0 / 5.7	7.1 / 7.1 / 6.8	6.5 / 7.1 / 6.8	9.1 / 6.0 / 5.6
young	7.6 / 4.4 / 4.1	6.0 / 7.8 / 7.5	7.8 / 7.8 / 7.5	8.0 / 4.1 / 3.7
magnetar	7.6 / 4.4 / 4.1	6.4 / 8.1 / 7.7	8.2 / 8.1 / 7.7	7.1 / 3.2 / 2.9

Table 2: Maximum Lorentz factors γ_{max} for the three kind of particles: electrons / protons / iron nuclei. The value of the strength parameter at the light cylinder is also given.

launched by a rotating magnetic dipole. Instead we found a simple linear relation relating the strength parameter a_{B_L} to the Lorentz factor such that

$$\gamma_{max} \approx a_{B_L}. \tag{6}$$

This increase in the acceleration efficiency is imputed to the presence of a still strong radial component of the electric field which was absent in the study of [9]. The simulations performed in this section only followed a small number of particles due to the stringent computation time required to accurately evolve the particle velocity and position. Describing the plasma feedback onto the electromagnetic field would require a much larger number of particles coupled to the evolution of the electromagnetic field via Maxwell equations, leading to a particle-in-cell code. So far, although PIC codes exist and have been adapted to simulate neutron star magnetospheres, none was yet able to handle the parameter space explored in the present work.

4. Conclusions

Strongly magnetized rotating neutron stars are powerful and efficient particle accelerators able to accelerate leptons and hadrons to Lorentz factors as high as 10^9 for the former and slightly less for the latter. This upper limit remains largely independent on the nature of neutron star: millisecond pulsar, young pulsar or magnetar. We achieved these results by implementing realistic parameters in our particle pusher based on the exact solution of the LLR approximation of the equation of motion. Through extensive numerical tests, we show that our scheme is second order in proper time.

The simulation results are accurate and robust but at the expense of high computational cost because of the need to resolve the gyro-motion which is many decades smaller than the neutron star spin period. The radiation reaction limit regime offers a good compromise between accuracy and computational cost but the simplistic expression used is unable to reproduce all trajectories satisfactorily. Nevertheless, it could be conceivable to improve this expression by taking into account a finite Lorentz factor and special electromagnetic field configuration when the radiation

reaction is negligible due to a weak accelerating electric field. Nevertheless this extension is left for future work.

A straightforward implementation of the above pusher into a PIC code or codes is prevented by the fact that LLR uses the proper time as integration parameter. Its conversion into an inertial observer time is however feasible as shown by [8]. The next logical step would then be to shift from the test particle motion to a fully kinetic plasma simulation where the particle charge and current densities retroact to the electromagnetic field via Maxwell equations.

References

[1] Max Abraham. Prinzipien der Dynamik des Elektrons. *Annalen der Physik*, 315(1):105–179, 1902.

[2] Max Abraham. Zur Theorie der Strahlung und des Strahlungsdruckes. *Annalen der Physik*, 319:236–287, 1904.

[3] Arnim J. Deutsch. The electromagnetic field of an idealized star in rigid rotation in vacuo. *Annales d'Astrophysique*, 18:1, January 1955.

[4] P. A. M. Dirac. Classical Theory of Radiating Electrons. *Proc. R. Soc. Lond. Series A*, 167:148–169, August 1938.

[5] Lev Davidovich Landau and Evgeni Lifchitz. *Physique théorique : Tome 2, Théorie des champs*. Éditions Mir, Moscou, Éditions mir edition, 1989.

[6] H. A. (Hendrik Antoon) Lorentz. *The theory of electrons and its applications to the phenomena of light and radiant heat*. Leipzig : B.G. Teubner ; New York : G.E. Stechert, 1916.

[7] L. Mestel, J. A. Robertson, Y. M. Wang, and K. C. Westfold. The axisymmetric pulsar magnetosphere. *MNRAS*, 217:443–484, November 1985.

[8] J. Pétri. A relativistic particle pusher for ultra-strong electromagnetic fields. *J. Plasma Phys.*, 86(4):825860402, August 2020.

[9] J Pétri. Particle acceleration and radiation reaction in strong spherical electromagnetic waves. *MNRAS*, 503(2):2123–2136, May 2021.

[10] J. Pétri. Particle acceleration and radiation reaction in a strongly magnetised rotating dipole. *A&A*, 666:A5, October 2022.